Energy 54 (2013) 184–193

Contents lists available at SciVerse ScienceDirect

Energy

journal homepage: www.elsevier.com/locate/energy

A novel vertical axis water turbine for power generation from water pipelines

J. Chen [a,*], H.X. Yang [a], C.P. Liu [b], C.H. Lau [b], M. Lo [a]

[a] The Hong Kong Polytechnic University, Kowloon, Hong Kong, China
[b] Water Supplies Department, The Government of the Hong Kong SAR, China

ARTICLE INFO

Article history:
Received 10 September 2012
Received in revised form
27 December 2012
Accepted 31 January 2013
Available online 11 March 2013

Keywords:
Water pipeline monitor
Hydro power
Vertical axis water turbine
Drag-type
Lift-type
CFD simulation and experimental test

ABSTRACT

In order to help water supply utilities improve water supply management, offer early warning and control water pipeline leakage, so as to provide clean water to residents, many instruments are installed to monitor hydraulic and water quality conditions along the water pipelines. However, one of the challenges of such tremendous monitor system is its limited power resources to make the smart sensors and sensor networks operate continuously and safely due to poor site conditions. In this paper, a novel vertical-axis water turbine has been developed for hydropower harness inside water pipelines when extra water head can be consumed. The small hydro power generated can be used for power supply to the data collection systems in underground and congested locations or to maintenance work at remote locations. The device was developed through CFD (Computational Fluid Dynamic) simulation and lab tests. The performance of the developed water turbines and the flow characteristics inside water pipes were simulated using the ANSYS CFD packages: FLUENT and Gambit. After the simulation, a number of prototypes were fabricated and tested to measure the real power output and verify the simulated results. The results indicate that the simulation outcomes can offer a good guidance for the rotor design even though the difference between the simulation and experimental results is fairly large. The results also show that the rotor with a hollow structure combined with an eye-shaped slanted block in a pipeline could generate the maximum power as compared with other types of vertical-axis rotors. Furthermore, the simulation and test results of different generation turbines offer valuable information for developing hydropower harness device in confined conditions.

1. Introduction

Water is essential for life and plays a vital role in the proper functioning of the Earth's ecosystems [1]. Most of our daily water supply is offered by the water utilities which have to ensure the safe and clean water supply for local residents. Modern water utilities, however, are facing several challenges because many urban water pipelines installed during the rapid urban growth period after the World War II are now suffering from rapid deterioration [2]. The major challenges involve how to early warn and control water leakage, how to efficiently control and detect water quality, how to manage the pressure distribution along the pipeline, how to maintain and renew the pipeline and how to optimum design and operation of water distribution network. A large number of technologies and prediction models have been developed to deal with the challenges mentioned above during the past a few decades.

In terms of water leaking control, Rajani [3] and Kleiner [4] summarized the physically and statistically based models for structural deterioration prediction of water mains through model description, critique and data requirements. However, all these prediction models need a lot of data with different types. For example, the Frost load model [5] requires continuous freezing index, soil properties, thermal gradient at the freezing front, frost depth and other related variables. Based on the co-author's [6–8] publications of the Hadzilacos's [9] models, factors such as traffic load, frost load, earth load, pipe working and surge pressure, temperature change, internal and external pipe diameter and corrosion coefficients, bursting strength, tensile strength, maximum external load and fracture toughness have been taken into consideration in their probabilistic framework. Therefore, Rajani [3] and Kleiner [4] claimed that even the best physical analysis model is good only under the circumstance that relevant data are available for its implementation.

Water quality is another rising issue. The United states Environmental Protection Agency (EPA) claimed that microbes, chemicals, and pathogens are still a concern even EPA has set

* Corresponding author.
E-mail address: 09900589r@connect.polyu.hk (J. Chen).

0360-5442/$ – see front matter © 2013 Elsevier Ltd. All rights reserved.
http://dx.doi.org/10.1016/j.energy.2013.01.064

standards for about 90 contaminates. Levin [10] suggests that we need better, more efficient and sensitive monitoring tools and strategies, especially to assess microbial risks and groundwater contamination.

Most of these technologies and models are based on many types of data, enough detection nodes and synchronous and continuous data gained at one node for the analysis, inspection and prediction of the water leakage and quality so that water utilities need to install a lot of different types and quantities of sensors along pipelines to gain the different data for leaking and contamination inspections at different locations. Till now, most of the sensors are powered by batteries. However, the fact mentioned by the Younis [11] is that it is envisioned that monitoring network always need hundreds of nodes that operate on small batteries. According to Yang [12], the operation period per battery charge is only 21 day when an aqueous sensor network was applied to measure environmental parameters of interest for the lake or drinking water reservoir. Power supply to the data acquisition systems, especially the magneto elastic transmitter and sensor interface board, is usually off. Hence, they proposed to obtain power supply from the environment, such as thermoelectric and mechanical power. A real wireless sensor network was used by the Stoianov [13] to monitor the Boston city's water supply. Many sensors relied on battery operation due to the fact that many of the sensor locations do not have access to local utility grid power. Even using lossless data compression algorithms, the battery life (6 V 12 Ah battery) is about 50–62 days. They claimed that the major challenge in developing the wireless monitoring system [14] is how to balance the conflict between long distance, communication, bandwidth, local data processing and the constraints for low-power consumption.

Therefore, more and more studies have focused on how to provide power to the monitoring sensor networks which are the essential for the modern water mains management technologies and methods, especially for the sensors which have no access to grid power and need to offer continuous monitoring. In this paper, a new type of power supply system is proposed, which harvests a little hydropower from the pipeline for power supply to the data acquisition systems. This paper reports the development details of the micro hydropower system including CFD (Computational Fluid Dynamic) simulation and experiments.

2. Hydropower harvest inside the pipeline

In order to offer sufficient and safe power for the monitoring system, abundant hydropower inside pipeline seems very attractive. The superfluous water head or small part of kinetic hydropower inside pipeline can satisfy the power requirement of the monitoring system. But the challenge of using hydropower is to select a water turbine which can suit for the requirements of the water pipeline condition, especially for the underground and urban cities condition. The requirements are listed below:

- The average water velocity in the pipe is 1.5 m/s.
- Although some superfluous water head may exist in the water pipeline, the water turbine cannot consume a lot of water head to make sure drinking water can overcome pipe friction loss and can be delivered safely to the end user.
- At most of time, space for system installation is very limited in the underground condition and urban cities. Therefore, pathway of the water flow cannot be altered.
- The system does not have any underlying dangers that may affect water quality

There are many kinds of conventional water turbines which work at different water head and flow rate, such as Francis, Kaplan, Bulb and Pelton turbine. And the efficiency of those water turbines is normally range from 75 to 95 percent based on the size of hydro turbine generator aggregate.

According to Fig. 1 [15], Kaplan turbine looks like a promising turbine for the water pipeline because it can work at low flow rate and low water head condition. But Kaplan turbine will alter the pathway of water flow and cannot be well integrated with pipeline. Ampair's UW100 picohydro turbine which is a kind of bulb turbine was proposed by the Saftner [16] to generate the power for the wireless sensors. Although this kind of water turbine will not change the pathway of water flow, the generator and some electrical components were immersed in the drinking water. Any improper waterproofing of this system will contaminate the drinking water. And the loss of water head of this system also needs to be well evaluated. Thus Water Supplies Department (WSD) of the Hong Kong SAR Government has commissioned the Hong Kong Polytechnic University to develop a hydro turbine for pipeline applications which must satisfy the requirements mentioned above.

A vertical axis water turbine system shown in Fig. 2 was proposed to satisfy above requirements. By using such turbine, the pathway of water flow will not change, the electrical parts can be arranged outside of the water pipe, and there are some of ready-made tubular T joints which can be used directly on the pipeline. After searching the existing vertical axis turbines, lots of researches focused on the application of the vertical axis turbines in the open air or water condition [17–19]. A few of researchers have turned their interest to develop the vertical axis turbine used in the half [20–22] confined condition due to the fact that the Betz limitation can be broken. Several journal papers have been published about the vertical axis water turbine working in a complete confined condition. One company named Lucid Energy [23] developed a lift-type vertical axis water turbine for the big water pipeline recently. Fig. 3 shows this kind of lift-type vertical axis water turbine. And this system is only developed for the pipelines which is bigger than 24 inch. Therefore, the fact is that there is very little information about the vertical axis water turbine used in a confined condition, especially for the small pipelines. In this paper, we want to develop the vertical axis water turbine for 100 mm pipeline to convert as much as possible energy when the average water velocity is 1.5 m/s and the water head drop is less than 5 m.

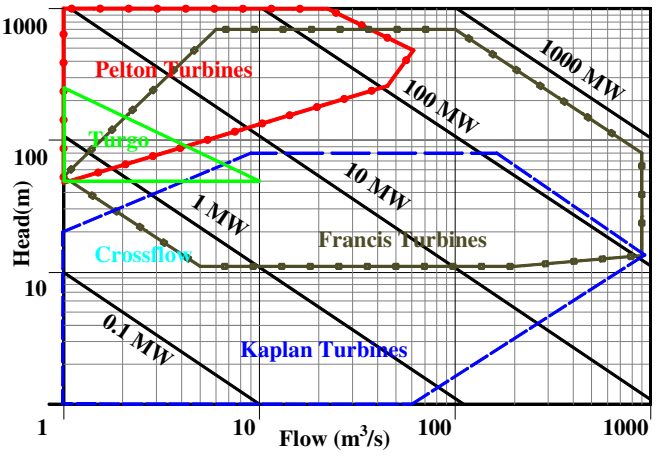

Fig. 1. Turbine application chart.

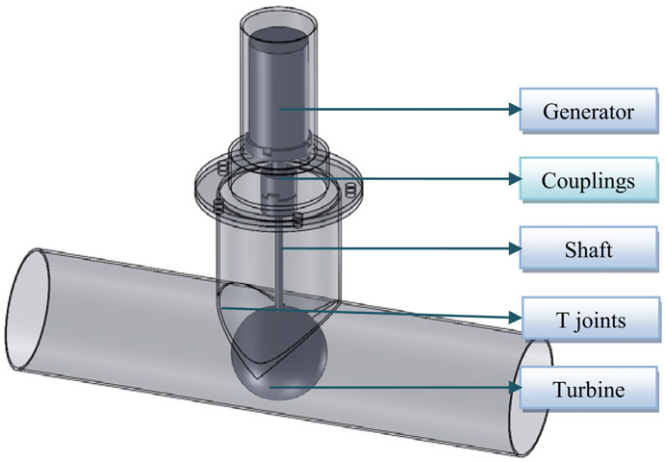

Fig. 2. The proposed system for the water pipeline.

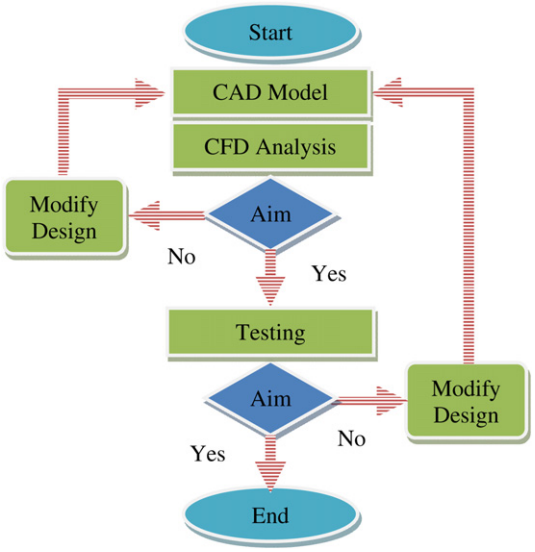

Fig. 4. Design methodology.

3. Design of the hydropower system

3.1. Design process

Due to the development of the CFD, the modern fluid mechanical design is changed from pure experimental design to simulation-based design supplemented by experimental test. This design process is described in Fig. 4, which can be divided into two stages. In the first stage, the proposed water turbine was made using the CAD software, then the CAD model was imported into the CFD software to simulate different water turbines' performance under different working conditions. After that, the simulation results were compared to the design aims to check whether the performance of the proposed model can meet the design aims. If the performance of the proposed model cannot meet the design aims, then the first two processes were repeated till the performance of the proposed turbine achieves the design aims.

Once the simulated performance of the proposed model was close to the design aims, the testing stage was launched. If the performance of the proposed model cannot meet the design aims, the first and second stage will be repeated until the model meets the requirements. There are mainly two purposes of the experiments, i.e. to ensure that the proposed models meet the design requirements, and to find whether the simulation is really instructive and the difference between the experimental results and simulation results.

3.2. CFD settings

The design and prediction capacity of the CFD has been confirmed to be effective and instructive in many areas, such as fluid machinery, aerospace and atmospheric environment and other fields. The CFD method also has been widely used in the design of the vertical axis wind turbine [24–26]. In this paper, the ANSYS CFD package, which is considered to be one of the best fluid design software packages nowadays, is applied to simulat the vertical axis water turbine. To simulate the unsteady flow field, the sliding mesh method was adopted. The computational domain was divided into internal and external parts. The face between the internal and external domain is defined as an interface which allows the flow properties to transport through the interface. A simple algorithm was used to solve the Navier–Stokes equations. The enhanced wall treatment was chosen for the near-wall region to resolve the viscous layer and the Y+ of the turbine blades should be close to 1. The whole computational domain was decomposed by 1.5 million unstructured tetrahedral meshes.

The mesh of the final design is presented in Fig. 5. Although the mesh number remains a controversial issue, the degree of the mesh number was considered well enough for such a small computational domain to make an investigation of the grid-dependence unnecessary. And the computational time of such one case is about one day using a desktop computer with Intel Core2 Quad CPU Q9550 @ 2.83 GHZ 2.83 GHZ processor. It means that we need four days to get one turbine's power coefficient curve at four different rotational speeds. That is why some simulations of the water turbines only have one or two power coefficient points.

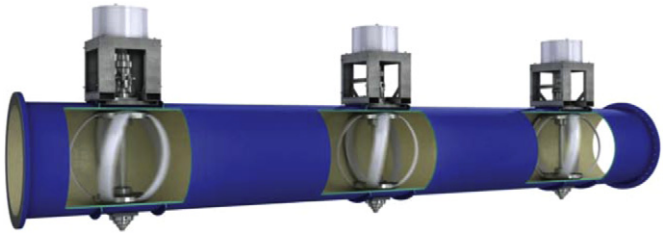

Fig. 3. Lucid energy lift-type turbines.

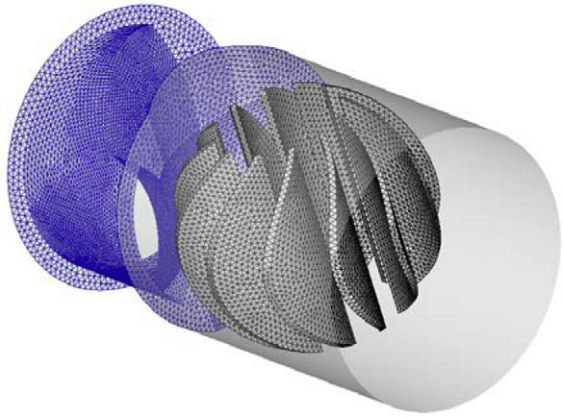

Fig. 5. Detailed mesh of the simulated models.

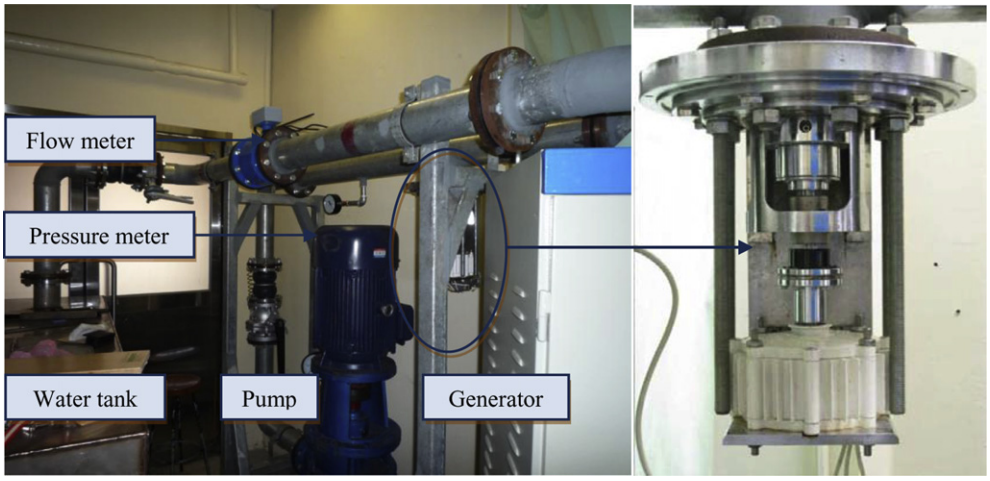

Fig. 6. Whole testing rig.

It is unfortunate that none of turbulence model can be applied to all the problems. The choice of the turbulence model depends mainly on the considerations such as the physics encompassed in the flow, the required level of accuracy, the available computational resources, and the amount of time available for the simulation. Taking into account the available computing resources, the number of the design models and relative shorter design cycles, a two-equation model is chosen to approach the Reynolds-averaged Navier-stokes equations. The most commonly used turbulence model is the $\kappa-\varepsilon$ turbulence model, and the realizable $\kappa-\varepsilon$ model is likely to be superior to the standard $\kappa-\varepsilon$ and RNG $\kappa-\varepsilon$ models for flows involving rotations, boundary layers under strong adverse pressure gradients, separation, and recirculation. Another kind of the two-equation turbulence models is the $\kappa-\omega$ models. Among the $\kappa-\omega$ models, the SST $\kappa-\omega$ model is more reliable and accurate than the standard $\kappa-\omega$ model due to the additional features added into the SST $\kappa-\omega$ model [27]. According to the above analysis, the SST $\kappa-\omega$ model and realizable $\kappa-\varepsilon$ model were adopted to simulate the initial case. The default values in Fluent are used for all the constant values of the SST $\kappa-\omega$ and realizable $\kappa-\varepsilon$ model. Velocity inlet was used for the inlet of pipeline. The velocity of the flow is 1.5 m/s according to the datum provided by the Water Supply Department of the Hong Kong SAR Government. The outlet of pipelines is the pressure outlet boundaries of the model. It is found that there is no significant difference between the simulation results of the two models over a large number of time steps. Therefore, we selected the realizable $\kappa-\varepsilon$ model to simulate all the subsequent design models.

In order to calculate the power output, the torque coefficient of the water turbine is monitored. The average torque coefficient will be calculated until the toque coefficient shows periodic variation. To evaluate the pressure drop caused by the water turbine, the monitoring point of the inlet pressure and outlet pressure were placed upstream 4 times and downstream 8 times diameter of the pipeline, respectively.

3.3. Prototypes and experiment setup

The simulated water turbine was fabricated by a Computer Numerical Control (CNC) machine using stainless steel which will not contaminate drinking water and has enough strength. The prototype water turbine was installed into a lab testing system as shown in Fig. 6 to measure the real performance of the developed turbine. The testing system is mainly composed of a water tank of 1.6 m^3, a circulation pump, valves and sensors in a circulation loop. The pump is assumed to operate at 50% of its full capacity during the 8–10 h final acceptance test. A 37 kW pump produces 82 m water head at 81 m^3/h (equivalent to 2.8 m/s in a 100 mm pipe) to simulate the real water pipeline conditions. A variable speed drive will control the revolution speed of the pump. Several valves were used to regulate the water pressure and flow rate. There are also several sensors used to monitor the flow rate, temperatures and pressures inside the pipe. The flow meter was placed far away from the water turbine. The inlet and outlet pressure sensors were installed upstream 5 times and downstream 4 times diameter of the pipeline, respectively, due to the limited space in our lab. If 5 m water head is consumed totally, the estimated power is $\alpha \times 384.8$ W, where α is the block ratio which is defined as the ratio between the turbine's diameter and the diameter of the pipeline. If the water turbine is well designed, it will produce at least 80w power when the assumptive system efficient is 0.3 and α is 0.7. The following equation is used to estimate the potential power generation of the water turbine:

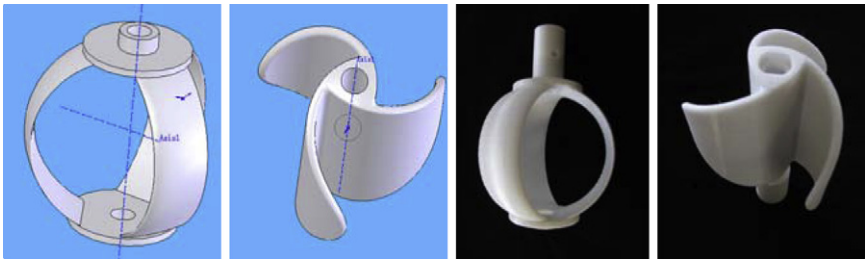

Fig. 7. Initial proposed designs.

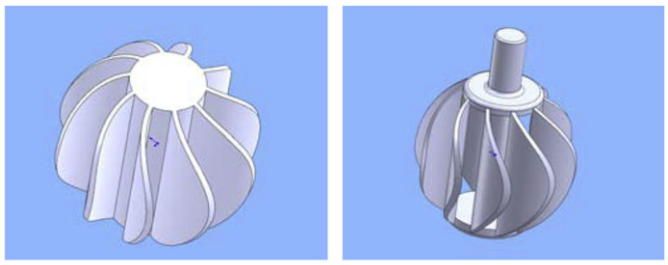

(a) Solid turbine (b) Hollow turbine

Fig. 8. The solid and hollow drag-type turbines.

$$P = \rho g\left(z_1 + \frac{p_1}{\rho g} + \frac{v_1^2}{2g} - z_2 - \frac{p_2}{\rho g} - \frac{v_2^2}{2g}\right)Q$$

Therefore, a micro permanent magnet power generator (FF-50 W) was used due to the propriety of low starting torque and zero cogging design whose rated power output is 50 W and maximum output can reach 100 W. In addition, the generator winding would be customized finally after testing the system performance, such that the output voltage at the maximum power point can match the battery charging voltage, which is around 28 V.

4. Experimental and simulation results of the three evolutions

4.1. First generation of the hydropower system

According to literature survey, there are very few reports about the vertical axis water turbine working in a confined condition [20,28]. Thus, there is little reference which can be found for this project. Therefore, in the initial design stage, different spherical drag and lift-type water turbines which are mainly based on the vertical axis wind and water turbines were proposed and simulated using the CFD software. The airfoil used was the NACA 4415 airfoil which is considered as a promising airfoil for the Darrieus rotor [29]. The drag-type turbine was a conventional Savonius rotor with three blades and zero overlap. Some of the proposed models (left) and real models (right) are shown in Fig. 7.

The design parameters of the lift-type turbines are their chord length and blade number. The rotor size and blade number are the design parameters of the solid drag-type turbines. The diameter of the hollow circular cylinder is the design parameter of the hollow drag-type turbines. Fig. 8 shows the difference between the solid and hollow turbines. All the results of simulated and testing cases were numbered. A letter S will be added before the simulated case number. Similarity, a letter T means testing. If one case was simulated and tested, both S and T will be used in the case number.

Table 1 shows the simulation results of the four different lift-type vertical water turbines at different rotational speeds. In order to improve the self-start ability, the lift-type turbine with high solidity was used. The rotational speeds of the lift-type turbines were initially decided according to the principle of the high solidity vertical axis wind turbine in open conditions. The higher solidity, the sharper the power curve is [30]. In order words, the maximum power point of the turbine is close to lower tip speed ratio (TSR). Thus, the evaluated TSR for the turbine ranged from 0 to 4. The interval between the two TSR points was 0.4. After the simulation, we found that the power coefficient is negative when the TSR is larger than 2.5. Therefore, the TSR of most of the simulation cases is less than 2.5. The TSR is defined as:

$$\lambda = \frac{\omega^* r}{v}$$

Where v is the water velocity, ω is angular speed and r is the radius of the turbine. The solidity is expressed as:

$$\sigma = \frac{N^* c}{D}$$

Where N is the blade number of the turbine, c is chord length of the airfoil and the D is the diameter of the rotor.

Comparison between the case S1 and case S2 shows that the chord length influence on the turbine performance is obvious. The conclusion drawn from the comparison is the same as that of a vertical axis wind turbine in the open condition. The higher solidity, the sharper the power curve is. The reason why the working principle is the same between a wind turbine and a water turbine may be that the rotor blockage value is not big enough to influence

Table 1
Simulation and testing results of the lift-type model.

	Case No.	Blade No.	Chord length/ solidity (mm)	Angular speed/TSR (rad/s)	Power output (W)	Pressure drop (pa)
Simulated lift turbine diameter (66 mm)	S1	3	24/1.09	18.75/0.4	0.65	1101
				37.5/0.8	1.86	682
				56.25/1.2	3.14	1001
				75/1.6	1.28	915
	S2	3	32/1.45	18.75/0.4	0.48	749
				37.5/0.8	1.568	927
				56.25/1.2	0.22	*
				75/1.6	0.027	2495
	S3	5	16/1.21	37.5/0.8	1.4	3025
				56.25/1.2	1.65	3342
	S4	6	24/2.18	37.5/0.8	1.14	2223
				56.25/1.2	2.06	2560
Testing result	T1-S1	3	24/1.09	*	0	*
	T2-S2	3	32/1.45	*	0	*

Table 2
Simulation and testing results of drag type models.

	Case No.	Blade No.	Rotor size (mm)	Angular speed (rad/s)/TSR	Power output (W)	Pressure drop (pa)
Simulated drag turbine (solid)	S5	3	66	37.5/0.825	0.543	1551
	S6	3	86	22.5/0.645	3.8	6777
				30/0.86	4.28	7030
				37.5/1.075	4.2	7268
	S7	3	95	22.5/0.7125	10.64	*
				30/0.95	12.34	*
				37.5/1.1875	13.59	*
				45/1.425	14.49	*
Test result	T3-S6	3	86	*	0	0

Table 3
Simulation and testing results of drag type models.

	Case No.	Blade No.	Rotor size (mm)	Angular speed (rad/s)/TSR	Power output (W)	Pressure drop (pa)
Simulated drag turbine (solid)	S8	3	66	37.5/0.825	0.543	1551
	S9	5	66	18.75/0.4125	1.875	7829
				28.125/0.618	3.9375	8173
				37.5/0.825	0.85	*
	S10	10	66	150.33	3.67	7752
				22.5/0.495	4.63	7344
				30/0.66	5.24	7086
				37.5/0.825	4.8	6833

Table 4
Simulation and testing results of drag type models.

	Case No.	Blade No.	Diameter of hollow circular cylinder (mm)	Rotor size (mm)	Angular speed (rad/s)/TSR	Power output (W)	Pressure drop (pa)
Simulated drag turbine (hollow)	S11	10	20	92	15/0.46	3.06E-04	137,200
					30/0.92	9.65E-05	137,200
	S12	10	30	92	15/0.46	2.92E-04	95,746
					30/0.92	1.01E-04	97,314
					40/1.22	−3.31E-05	*
					50/1.53	−1.69E-04	*
	S13	10	40	92	15/0.46	1.01E-04	68,600
					30/0.92	−2.59E-04	71,736

the working principle of the vertical axis turbine in the open condition. The comparison of the case S3 and case S4 shows the blade number influence on the turbine performance. The power output of the case S3 and case S4 is much lower than that of the case S1. However, the pressure drop of the case S3 and case S4 is much sharper than the case S1 and case S2, although the pressure drop of the case S2 is not shown at angular speed 56.25 rad/s because the datum was lost one year ago due to the damaged of a hard disk. The case S1 and case S2 were fabricated and installed into the pipeline to measure their real power outputs. The last two rows in Table 1 show the testing results of the case S1 and case S2. Zero power output is predictable when the case S1 and case S2 were used to drive the 50 W power generator.

The optimum TSR of the drag-type turbines is about 0.8 in the open condition. Thus, the angular speeds of the drag-type turbines can be chosen when the TSR is close to 0.8. Table 2 shows the influence of the rotor size on the power output of the solid drag-type turbines. It is obvious that the power output increase with the increase of the rotor size. The highest power output is 14.49 W for the case S7. The power output increase could be probably attributed to several factors. The power output is in direct proportion to the sweep area of the turbine in the open condition. It seems that this principle is applicable to confined condition. However, the power changes non-linear along the sweep area. A small change of the sweep area could cause big changes of power output. The second factor is the block ratio which is only used in the confined condition. Water flow can skirt around the turbine in the open condition, but it can only act on the water turbine directly due to the limitation of the pipe wall, thus generating more thrust force.

The influence of the blade number on the power output of the solid drag-type turbines is presented in Table 3. It is clear that the more blades a turbine has the more power it can generate. The maximum power output is 5.24 W when ten blades are adopted for the solid drag-type turbine working at 30 rad/s. In the open condition, the power coefficient will decrease with the increase of the blade number. However, it is opposite in the confined condition. The reason for this increase may be that the numbers of advancing blades which generate the thrust forces is increased in the confined condition. And the drag force produced by the returning blades is reduced due to the smooth pass of the incoming flows. Three turbines with different diameters of hollow circular cylinder were presented in Table 4. It is found that the power output is almost close to zero when the water velocity is 1.5 m/s and the pressure drop is very high. One possible reason, which is responsible for this phenomenon of lower power output and high pressure consumption, is that the angular speed of the rotor is evaluated improperly. The optimum rotational speed of this hollow rotor with multiple blades may be much lower than the rotational speed of estimation. Hence, this rotor is working at off-design condition which causes turbulence flow in and around turbines. Another reason may be that this type of turbine is not suit for this design conditions.

Comparison between Tables 1–4 shows that the power output of the drag-type turbine is generally higher than that of the lift-type turbines and the same for the pressure drop in a confined condition except for the hollow drag-type turbines, which indicates that the solid drag type especially ones with more blades and larger diameter, is more suitable than the lift-type in a confined space. Although the power output of the first generation of the hydropower generators is sufficient enough for the power of the monitoring sensors, there is still a lot of room for improvement due to the pressure drop of the initial proposed turbine which is much lower than the allowed pressure head consumption of 5 m. Further modification is necessary for the drag-type turbines so as to generate more power.

4.2. Second generation of the hydropower system

Based on the conclusions drawn from the development of the first generation turbines, more attention was paid to the drag-type turbines with more blades and larger size on their second generation as more water head need to be consumed to have more power output. According to the working principle of the drag-type rotor, it is obvious that the returning blades of the drag type turbine create most of the resistance force. If we can install a block inside the pipeline to surround the returning blades, the water flow will not attack the returning blades directly. At the same time, part of the water head energy is converted into kinetic energy due to narrowing the water flow channel. The returning blades, advanced blades and some blocks are shown in Fig. 9.

Therefore, four types of blocks were designed for solid drag-type turbines. Fig. 10 shows the four types of blocks according to sequence of the evolution. In order to install the block through the T joints, the size and type of the blocks are restricted. From left to right in Fig. 10, the vertical block is the first proposed block which can directly be inserted into the pipeline through a T joint. The second block which is a long slanted block needs to be divided into three pieces for installation. Hence, the installation process of the

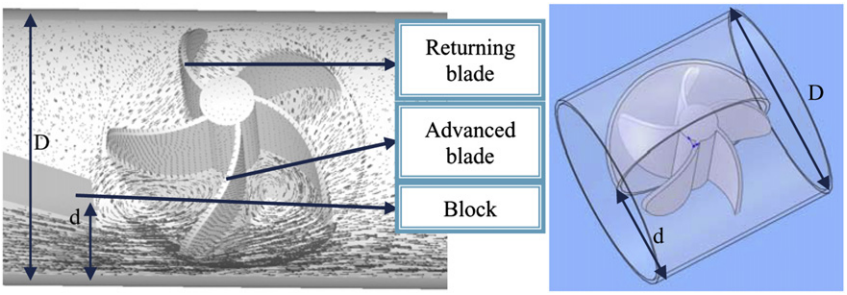

Fig. 9. The working principle of the drag-type turbine.

Fig. 10. Four types of the blocks.

second block is relatively complex. Thus, the third block which is a short slanted block was developed to replace the second block. The last block is a slanted block with an eye-shaped opening. The definition of the block ratio which is shown in Tables 5 and 6 is the same for the vertical, long slanted and short slanted blocks. The block ratio is defined as d/D which is presented in Fig. 9. The block ratio of the eye shaped block is defined as the ratio of outlet area to inlet area. The angular speed of the simulated turbines was evaluated based on the first generation turbine.

The simulation results of the vertical and slanted blocks are listed in Table 5 and the test results are presented in Table 6. Case S14 and case S15 were compared to investigate the blades number influence on the turbine performance when the block ratio is 0.5. It is found that power output of case S14 is less than that of the case S15 when the vertical block is combined with solid turbine. The maximum power output of the case S14 is 10.6 W, which seems that the principle (more blades for more power) is suitable for the vertical block when the block ratio is 0.5. The corresponding tested turbine is the case T5 which has zero power output. More tested cases with vertical block were listed in Table 6. The increase of the block ratio leads to power output increase. The maximum power output and pressure drop are 13.4 W and 3.75 m, respectively, when the blade number is six and block ratio 0.9. As the power output is much less for the vertical block arrangement, a different block was developed and simulated. Based on the test results of the vertical block, the simulation of the second block focused on the high block ratio. Although the simulation results shows that the maximum power output is 67.69 W when the block ratio is 0.8, the test result of power output is only 11.8 W.

It is a little complex to install the long slanted block through the T joint therefore a shorter slanted block was developed and tested. It seems that the power output of the short slanted block is close to

Table 5
Simulation results of drag type models.

	Case No.	Blade No.	Block type block ratio	Rotor size (mm)	Angular speed (rad/s)	Power output (W)	Pressure drop (pa)
Simulated results of drag turbine (solid) + vertical block or long slanted block	S14	5	Vertical block 0.5	86	37.5	2.2	4007
					56.25	10.6	5726
	S15	10	Vertical block 0.5	86	15	3.67	*
					22.5	4.63	*
					30	5.24	7305
					37.5	4.8	6994
	S16	5	Long slanted block 0.6	86	30	12.56	36,829
					40	13.77	36,339
					50	12.29	36,004
	S17	5	Long slanted block 0.8	92	30	55.15	84,523
					40	64.68	85,176
					50	67.69	80,875
	S18	6	Long slanted block 0.8	92	37.5	59.79	87,623
	S19	10	Long slanted block 0.8	92	40	64.43	85,329

Table 6
Testing results of drag type models.

	Case No.	Blade No.	Block type	Rotor size (mm)	Max Power output (W)	Pressure drop (pa)
Testing results drag turbine (solid) + four kinds of blocks	T4	3	Vertical block 0.5	86	0	*
	T5-S14	5	Vertical block 0.5	86	0	*
	T6	5	Vertical block 0.7	86	0	*
	T7	5	Vertical block 0.8	86	1.9	21,952
	T8	6	Vertical block 0.7	86	1.1	20,678
	T9	6	Vertical block 0.8	86	4.0	23,226
	T10	6	Vertical block 0.9	86	13.4	36,750
	T11-S17	5	Long slanted block 0.8	92	11.8	*
	T12	5	Long slanted block 0.9	92	0	*
	T13	5	Short slanted block 0.8	92	12	*
	T14	5	Slanted block with eye-shaped opening 0.9	92	24.8	54,880
	T15	6	Slanted block with eye-shaped opening 0.8	92	6.1	32,928
	T16	6	Slanted block with eye-shaped opening 0.85	92	26.2	46,550
	T17	6	Slanted block with eye-shaped opening 0.9	92	32.2	57,036
	T16	6	Slanted block with eye-shaped opening 0.95	92	26.6	102,018

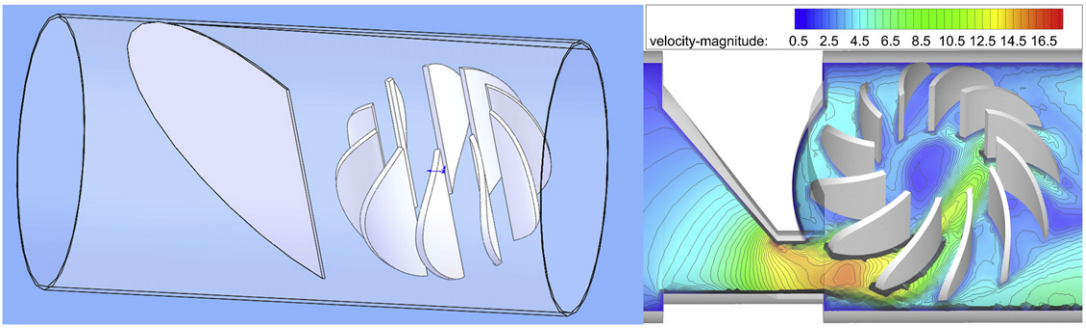

Fig. 11. Two different combinations.

that of the long slanted block. Three blocks mentioned above have a common disadvantage, i.e. the offset between the flow pathway and the turbine's advanced blade blocking will increase when the block ratio increases. Thus, the fourth generation block was developed. Through this new block, the flow can act directly on the turbine's advanced blades. Fig. 10 illustrates this improvement clearly. The eye shaped block was manufactured and tested without further simulation. From Table 6, the maximum power of the slanted eye shaped block can reach 32.2 W. This is a significant improvement and more water head was consumed. The optimum block ratio is 0.9.

4.3. Third generation of the hydropower system

In fact, the power output from the above turbines is enough to supply the monitoring system. However, there is still much room for improvement according to the estimation. From the above simulation and tests, it is found that the solid drag turbine can produce more power for the first generation of the water turbine and the slanted eye shaped block is the best block in the second generation. After testing different design combinations of the solid turbines and blocks, the only combination which is not tried is the hollow turbine with a block due to the zero power output of the hollow drag type turbines in the first generation.

The simulation of this new combination is thus carried out. Two types of the combinations are presented in Fig. 11. One is the combination of a long slanted block and a hollow drag type turbine. Another one is the combination of the slanted eye shaped block and hollow drag type turbine.

Table 7 shows the simulation results. The power output of the case S22 is twice higher than that of the case S19 which produces the highest power in the second generation. The only difference between the two cases is the turbine's hollow structure. The simulation results indicate that the optimum diameter of the hollow circular cylinder is close to 45 mm. From the conclusion of the second generation development, the best block is the slanted eye shaped turbine. Thus, the hollow turbines were used together with a slanted eye shaped block. Case S23 and case S24 show the influence of the turbine diameter with a hollow circular cylinder. Only two kinds of diameters were investigated of the slanted eye shaped block due to time consideration and some indications given from the simulation of the long slanted block system. The influence of blade number can be found through the comparison among the case S24, case S25 and case S26. The simulation results show that the optimum blade number is close to 15. In fact, the difference of the simulation power output between the 12-blades turbine and 15-blades turbine is only 2 W. Although the combination of the hollow turbine and slanted eye shaped block provides a significant improvement of power output, the water head loss is close to 12 m which is not acceptable. In order to validate the conclusion about the blade number influence, the turbines with large blade number difference were developed. The test results presented in Table 8 are very inspiring. The maximum power output of this combination reached 88.2 W and the consumed water head is within the 5 m limit. The optimum blade number of the tested turbines is 12 which have also validated the conclusion drawn from the simulation results, although the power output and pressure drop from the simulation are much higher than the power output and pressure drop of the test results.

Table 7
Simulation results of drag type models.

	Case No.	Blade No.	Block type	Diameter of hollow circular cylinder (mm)	Rotor size	Angular speed (rad/s)	Power output (W)	Pressure drop (pa)
Simulated results of drag turbine (hollow + long slanted block or slanted eye shaped block	S20	10	Long slanted block 0.8	20	92	40	99	72,787
	S21	10	Long slanted block 0.8	30	92	40	116.3	74,739
	S22	10	Long slanted block 0.8	45	92	40	127.5	75,647
	S23	12	Slanted block with eye-shaped opening 0.9	45	92	40	226.8	124,337
	S24	12	Slanted block with eye-shaped opening 0.9	55	92	40	215.3	124,369
	S25	15	Slanted block with eye-shaped opening 0.9	45	92	40	228	122,469
	S26	18	Slanted block with eye-shaped opening 0.9	45	92	40	221	122,642

Table 8
Testing results of drag type models.

	Case No.	Blade No.	Block type	Diameter of hollow circular cylinder (mm)	Rotor size (mm)	Angular speed (rad/s)	Power output (W)	Pressure drop (pa)
Tested results of drag turbine (hollow) + slanted eye shaped block	T17	8	Slanted block with eye-shaped opening 0.9	45	92	66	66.4	43,904
	T18-S23	12	Slanted block with eye-shaped opening 0.9	45	92	74	88.2	47,530
	T19	24	Slanted block with eye-shaped opening 0.9	45	92	63	67.4	43,414

Fig. 12. The hydropower system is running on site.

4.4. Summary of the three generations

A summary of the typical vertical axis water system is presented in this section. The power output is increased significantly from zero to 88.2 W during the one-year experiment test and CFD simulation. The typical designs of the different generations are listed below.

The combination of the hollow drag type turbine and the slanted eye shaped block not only can produce the estimated power to supply the monitoring system, but also satisfy the power supply requirements. The eye shaped block and hollow turbine can be inserted easily through the T joints on the pipeline. The power output and pressure drop can be controlled through the adjustment of the block ratio, which makes the system readily suitable to the different requirements.

Drag type turbine design		Max power (W)	Head drop (m)
1st gen: 5-blade solid turbine (∅86 mm) + vertical half block		0	0
1st gen: 5-blade solid turbine (∅92 mm) + 80% short slanted block		12.0	N/A
2nd gen: 6-blade solid turbine (∅92 mm) + 90% slanted eye shaped block		32.2	5.82
3rd gen: 12-blade (∅92 mm) hollow turbine + 90% slanted eye-shaped block		88.2	4.85

Although the simulated and testing results demonstrate large quantitatively difference, the trends and variations of the simulated results are consistent with that of the testing results from the qualitative point of view. Both the simulation and test results show that the rotor with hollow shaft and short slanted block can generate much more power than the others. The simulation results do offer important theoretical guidance for the design of a real model. The possible reason for the difference is that the energy losses caused by water flow friction and various mechanical frictions were not considered in the simulations, and the mismatch between the turbine's power curve and generator's power curve may exist. Besides, the simulated models and water pipe are not exactly the same as the tested models and water pipe in shape. In addition, the effect of the CFD settings on the simulation results is not well investigated profoundly due to the high cost of computational effort and the limitation of design time.

5. Conclusions

An inline vertical axis water turbine is developed in this paper for power supply to water pipeline data monitoring systems. This turbine system is designed for a 100 mm pipeline. The expected power output is larger than 80 W when water velocity is 1.5 m/s and pressure drop is less than 5 m. After simulating and testing more than 20 different kinds of water turbines under various working conditions, the combination of the vertical axis water turbine with a hollow shaft and a short slanted eye shaped block was proved to be the best for generating the highest amount of power output which is 88.2 W. Further improvement can still be made for this novel inline vertical axis water turbine although the final design can meet the expectations under certain limitation. The design parameters which need to be further investigated can be the tilted angle of the turbine blades, folium of turbine blades and the hollow shapes of the turbines. Lastly, the simulated and testing results offer valuable insight into hydropower harvest inside the water pipeline of different sizes, although the system developed in this paper focused on the 100 mm pipeline. Some of the turbines of the first and second generations may also be adopted when power supply demanding is low.

Several final systems have been installed at designated areas in Hong Kong for the purpose of further on-site investigation. One of these systems is presented in Fig. 12. The measured value of the on-site power output is very close to the tested value in laboratory.

Acknowledgments

The work described in this paper was supported by the Water Supplies Department and the Inter-Faculty Research Grant of The Hong Kong Polytechnic University (Project No.: G-YG08). The PolyU Technology & Consultancy Company Limited provided a lot of laboratory testing support to the project.

References

[1] Learn the issues: water. United States Enviromental Protection Agency; 2012.
[2] Brothers K. A practical approach to water loss reduction. Water 2003;21:54–5.
[3] Rajani B, Kleiner Y. Comprehensive review of structural deterioration of water mains: physically based models. Urban Water 2001;3(3):151–64.
[4] Kleiner Y, Rajani B. Comprehensive review of structural deterioration of water mains: statistical models. Urban Water 2001;3(3):131–50.
[5] Rajani B, Zhan C. On the estimation of frost loads. Canadian Geotechnical Journal 1996;33(4):629–41.
[6] Camarinopoulos L, Chatzoulis A, Frontistou-Yannas S, Kallidromitis V. Structural reliability of water mains. In: Proceedings of the probabilistic safety assessment and management 96: ESREL 96-PSAM-III; Crete, Greece, 1996(a).
[7] Camarinopoulos L, Pampoukis G, Preston N. Reliability of a water supply network. In: Proceedings of the probabilistic safety assessment and management 96: ESREL 96-PSAM-III; Crete, Greece, 1996(a).
[8] Camarinopoulos L, Chatzoulis A, Frontistou-Yanas S, Kalidromitis V. Assessment of the time-dependent structural reliability of buried water mains. Reliability Engineering and Safety 1999;65(1):41–53.
[9] Hadzilacos T, Kalles D, Preston N, Melbourne P, Camarinopoulos L, Eimermacher M, et al. UtilNets: a water mains rehabilitation decision-support system. Computers, Environment and Urban Systems 2000;24(3):215–32.

[10] Levin RB, Epstein PR, Ford TE, Harrington W, Olson E, Reichard EG. US drinking water challenges in the twenty-first century. Environmental Health Perspectives 2002;110(Supplement 1):43.
[11] Younis M, Akkaya K. Strategies and techniques for node placement in wireless sensor networks: a survey. Ad Hoc Networks 2008;6(4):621–55.
[12] Yang X, Ong KG, Dreschel WR, Zeng K, Mungle CS, Grimes CA. Design of a wireless sensor network for long-term, in-situ monitoring of an aqueous environment. Sensors 2002;2(11):455–72.
[13] Stoianov I, Nachman L, Whittle A, Madden S, Kling R. Sensor networks for monitoring water supply and sewer systems: lessons from boston. In: Proceeding of the 8th annual water distribution system analysis symposium, Cincinnati, OH 2006, p. 1–17.
[14] Stoianov I, Nachman L, Madden S, Tokmouline T, Csail M. PIPENET: a wireless sensor network for pipeline monitoring. In: ACM/IEEE international conference on information processing in sensor networks. Massachusetts, USA: (MIT) Cambridge; 2007. p. 264–73.
[15] Water turbine chart; 2012.
[16] Saftner DA, Hryciw RD, Green RA, Lynch JP, Michalowski RL. The use of wireless sensors in geotechnical field applications. In: Proceeding of the 15th annual great lakes geotechnical/geoenvironmental conference, Indianapolis, IN; 2008.
[17] Kjellin J, Bülow F, Eriksson S, Deglaire P, Leijon M, Bernhoff H. Power coefficient measurement on a 12 kW straight bladed vertical axis wind turbine. Renewable Energy 2011;36(11):3050–3.
[18] Kirke BK, Lazauskas L. Limitations of fixed pitch Darrieus hydrokinetic turbines and the challenge of variable pitch. Renewable Energy 2011;36(3):893–7.
[19] Islam M, Ting DSK, Fartaj A. Aerodynamic models for Darrieus-type straight-bladed vertical axis wind turbines. Renewable and Sustainable Energy Reviews. 2008;12(4):1087–109.
[20] Kirke BK. Tests on ducted and bare helical and straight blade Darrieus hydrokinetic turbines. Renewable Energy 2011;36(11):3013–22.
[21] Ponta F, Dutt GS. An improved vertical-axis water-current turbine incorporating a channelling device. Renewable Energy 2000;20(2):223–41.
[22] Furukawa A, Watanabe S, Matsushita D, Okuma K. Development of ducted Darrieus turbine for low head hydropower utilization. Current Applied Physics 2010;10:S128–32.
[23] How it works. Portland: Lucid Energy.
[24] D'Alessandro V, Montelpare S, Ricci R, Secchiaroli A. Unsteady aerodynamics of a savonius wind rotor: a new computational approach for the simulation of energy performance. Energy 2010;35(8):3349–63.
[25] Raciti Castelli M, Englaro A, Benini E. The Darrieus wind turbine: proposal for a new performance prediction model based on CFD. Energy 2011.
[26] Mohamed MH, Janiga G, Pap E, Thévenin D. Multi-objective optimization of the airfoil shape of wells turbine used for wave energy conversion. Energy 2011;36(1):438–46.
[27] FLUENT A. 12.0/12.1 documentation users guide manual. Ansys Inc; 2009.
[28] Antheaume S, Maitre T, Achard JL. Hydraulic Darrieus turbines efficiency for free fluid flow conditions versus power farms conditions. Renewable Energy 2008;33(10):2186–98.
[29] Kirke BK. Evaluation of self-starting vertical axis wind turbines for stand-alone application [PhD]. Griffith Universtiy Gold Coast Campus; 1998.
[30] Paraschivoiu I. Wind turbine design: with emphasis on Darrieus concept. Presses Inter Polytechnique; 2002.